

## Experimental study of the influences of the pellet shape on the bulk density and the frictional behavior of polypropylene

Manuel Längauer, Christian Kneidinger, Keyan Liu, Gernot Zitzenbacher

University of Applied Sciences Upper Austria, School of Engineering and Environmental Sciences, Stelzhamerstraße 23, 4600 Wels, Austria

Correspondence to: M. Längauer (E-mail: Manuel.Laengauer@fh-wels.at)

**ABSTRACT:** Bulk solids are the raw material for almost every polymeric thermoplastic product. Their properties determine the quality of solids conveying and also influence the melting behavior of the material in processing units. This study investigates the influence of pressure and temperature on the bulk density of two thermoplastic polypropylene pellets of different shapes. Furthermore, the external friction dependent on temperature and pressure of those materials is examined at conditions usually occurring in the solids conveying zone of smooth barrel plasticating units. The experiments are carried out using a tribometer for polymer pellets which was adapted for these tests by making the sample chamber, the piston, and the cylindrical roll heatable. The tests show that long cylindrical pellets exhibit low bulk densities at low pressure and temperature, which can be increased dramatically—even above the values of spheroidal pellets—as those parameters increase. Moreover, the external coefficient of friction is always higher for the long cylinders and strongly dependent on the temperature. Those facts add up and can cause a higher output of single-screw extruders. © 2015 Wiley Periodicals, Inc. *J. Appl. Polym. Sci.* 2015, 132, 42197.

**KEYWORDS:** extrusion; friction; polyolefins; wear and lubrication

Received 15 December 2014; accepted 13 March 2015

DOI: 10.1002/app.42197

### INTRODUCTION

Single-screw extrusion (SSE) dates back many centuries and is nowadays used to fabricate polymeric products as sheets, pipes, and profiles. A screw is used to convey, compress, melt, pump, and homogenize plastic solids that are fed to the extruder. The most common shapes of bulk solids are powders or pellets. In polyolefin processing, pellet is the most widely used shape. Especially spheroidal pellets, as generated in hot-face pelletizing, are very popular. Cylindrical pellets are mostly manufactured in waterslide strand-cut pelletizers but they are not as common in polyolefin applications.<sup>1</sup> Bulk material properties have a significant influence on the extrusion process.<sup>2</sup> The shape and size of pellets determine those properties.

Extrusion experiments on a laboratory-scale single-screw extruder ( $D = 20$  mm) have been performed to analyze the influence of the pellet shape in regard to the mass flow rate and the processing conditions in a previous work.<sup>3</sup> They show that long cylindrical pellets exhibit a higher mass flow rate in all of the experiments while the counterpressure is comparable. For low screw speeds and high counterpressure, the achievable rise in the mass flow rate is 33%. The lowest increase is shown at high screw speeds and low counterpressure where it only accounted to 5.5%.

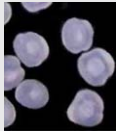
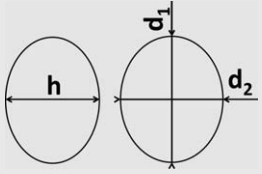

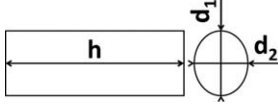
Screw-cool and pull-out tests were done to deliver information about differences in solids conveying and melting of the different pellet shapes. The long cylindrical pellets were highly compressed in the screw channel and stick together, even in the first turns.

Some other experimental studies also deal with the influence of bulk properties on extrusion.<sup>4,5</sup>

The reasons for the observed phenomena are found in the solids conveying behavior. In simulation, it has previously been assumed that the particles form a solid plug and behave as one large unit, rather than multiple small ones.<sup>6–11</sup> Newer studies approach this via the discrete element method, which can predict single particle flows.<sup>12–17</sup>

In the course of the development of solids conveying models, coefficients of friction and pressure anisotropy coefficients were implemented. The anisotropy coefficients had to be considered due to the anisotropic pressure propagation in the bulk material.<sup>18</sup> Coefficients of friction were needed in order to explain frictional heating and the inclination of the pellets to form a plug. One can differentiate between internal and external coefficients of friction (ECOF), the first describing the friction between the particles in a solid bulk, the latter the friction

**Table I.** Used Pellet Geometries and Their Dimensions

	Pellet shape	$d_1$ [mm]	$d_2$ [mm]	$h$ [mm]	Measured dimensions
	Virgin	$4.3 \pm 0.4$	$3.5 \pm 0.5$	$3.2 \pm 0.9$	
	Long cylinders	$2.3 \pm 0.3$	$1.9 \pm 0.3$	$6.3 \pm 0.2$	

$d_{1,2}$ : cross-sectional dimensions;  $h$ : length.

between the polymer and the enclosing system. In the case of SSE, the system is represented by the screw and the barrel surface. Since then, numerous approaches were made to investigate coefficients of friction of polymers to rework the mentioned calculation models.<sup>4,19–26</sup> Especially Chung *et al.* and Spalding and Hyun did basic work in this particular field with a device called a “Screw Simulator”.<sup>19,21</sup>

The most important properties of bulk materials in plasticizing extruders are their density and their ECOF. Internal friction is important when working with extruders with a grooved feeding zone.<sup>27,28</sup> The bulk density is strongly dependent on the shape of the single pellets.

The fact that the bulk density is also dependent on pressure and temperature was shown by Langecker *et al.* and Hyun and Spalding.<sup>29,30</sup> In Hyun and Spalding's experiments, a compaction testing cell with load cells on the top and the bottom was used to make the tests. Several different polymeric materials were used and a comparison between powders and pellets was made.

Only a few studies in literature deal with the influence of differently shaped polymer pellets of the same grade on the ECOF although none of them cover temperature dependence.<sup>3,19</sup>

In the aforementioned previous study, a major effect of the pellet shape on the external frictional coefficient could be demonstrated when working at standard conditions on a screw tribometer. It was found that long cylindrical polypropylene pellets exhibit a higher ECOF than spheroidal pellets.<sup>3</sup>

This study deals with the properties of two polypropylene pellet shapes of the same grade. One is a spheroidal virgin shape, generated in hot-face pelletizing, while the other is a long cylindrical shape that was made from the virgin material. The bulk density is first studied according to EN ISO 60. To demonstrate the effect of temperature, pressure, sample weight, time, and movement of the adjacent shaft on the bulk density of the two pellet shapes, a previously developed screw tribometer is used.<sup>31</sup> Several adaptations are made to allow heating of the shaft, the sample chamber, and the piston of the tribometer, in order to carry out experiments with different temperatures.

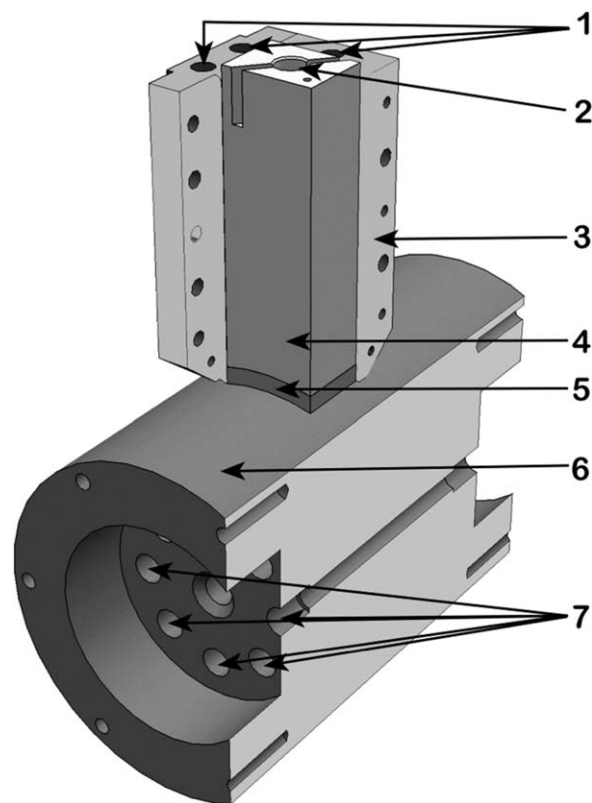
The ECOF between a monolayer of the pellets and a rotating polished tool steel shaft dependent on temperature and pressure

is examined with the screw tribometer. These experiments shall deliver possible explanations for the higher mass flow rate in the small-scale extruder and the fast pressure build-up when processing the long cylindrical pellets.

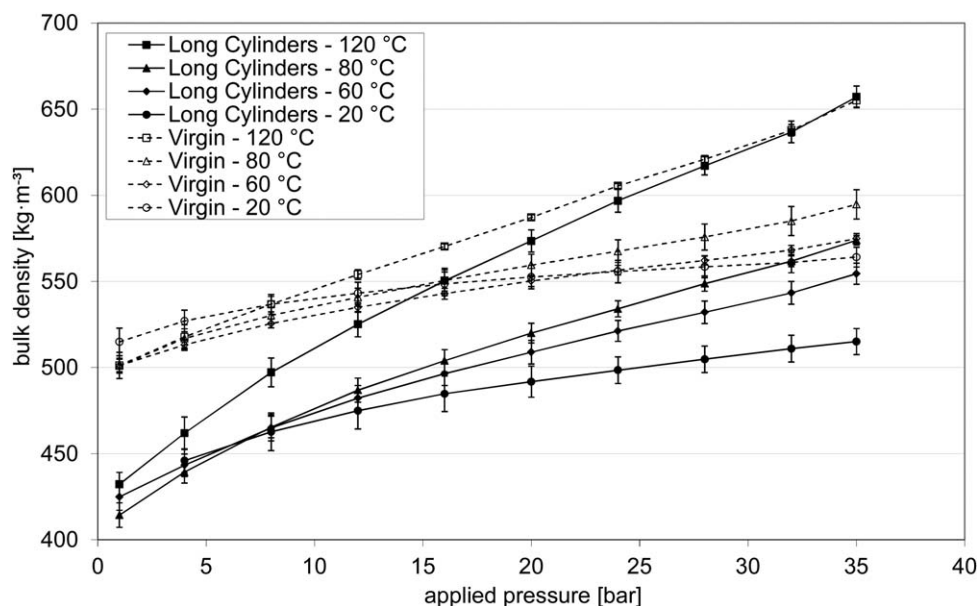
## EXPERIMENTAL

### Materials

The experiments were conducted using the polypropylene homopolymer type HD120MO produced by Borealis, Linz, Austria. Its major properties are a melt flow rate value of  $8 \text{ g} \cdot (10 \text{ min})^{-1}$



**Figure 1.** Detailed sectional view of the adapted screw tribometer. (1) Drill holes for heating cartridges in the sample chamber, (2) drill hole for heating cartridge in the piston, (3) sample chamber, (4) piston, (5) sample, (6) shaft, and (7) drill holes for heating cartridges in the shaft.



**Figure 2.** Bulk densities of the virgin material and the long cylinders at increasing pressure and a temperature of 20, 60, 80, and 120°C.

at 230°C and 2.16 kg, a density of 908 kg·m<sup>-3</sup>, and a tensile modulus of 1500 MPa.

Besides the spheroidal standard delivery geometry, a new long cylindrical shape was produced using a co-rotating twin-screw extruder type Thermo prism TSE 24 HC ( $D = 24$  mm;  $L/D = 28$ ) with a strand pelletizer. The temperature profile in this production process was set to 40°C (feed opening), 180, 190, 190, 200, 200, and 200°C (barrel heating zones) with a nozzle temperature of 210°C. The screw speed was 400 min<sup>-1</sup> with a torque of 37 N·m.

The different pellet geometries diverge in their dimensions as Table I shows. The dimensions of the cross-section ( $d_1$ ,  $d_2$ ) and the length of the pellets ( $h$ ) are measured.

Differential scanning calorimetry tests showed no significant difference between the heat flow plots of samples taken from the pellets.<sup>3</sup>

#### Determination of Solid Bulk Properties

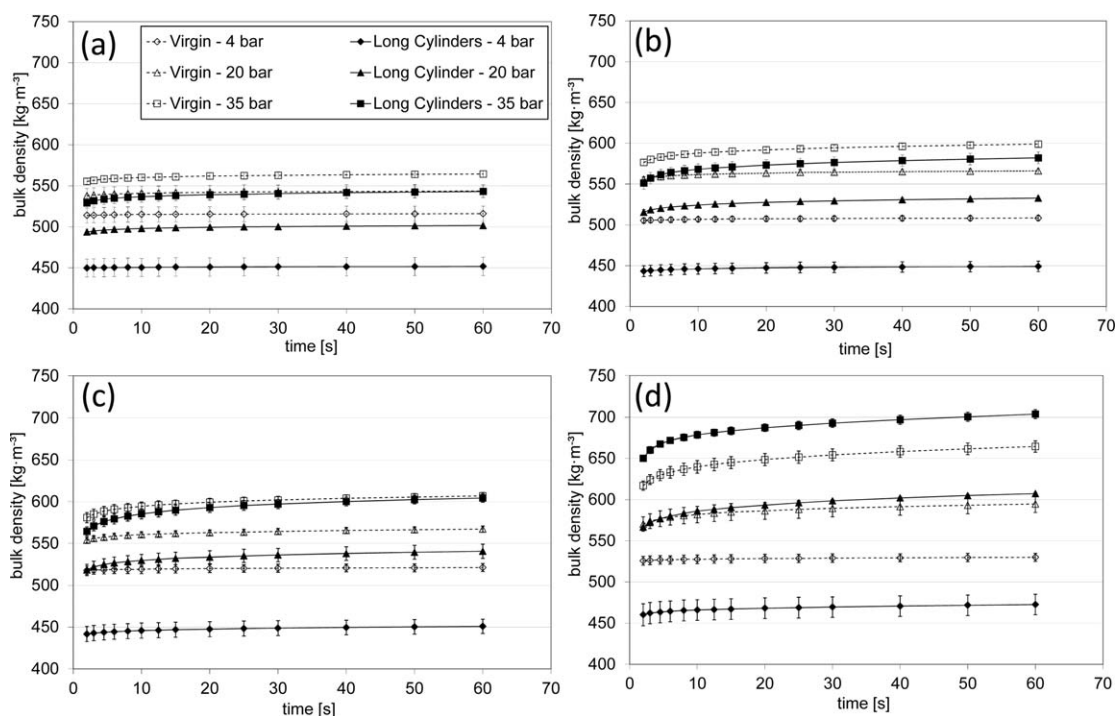
The apparent bulk density of the different pellet shapes was first measured at standard conditions using an apparatus according to EN ISO 60.

In order to investigate the effect of temperature and pressure on the bulk density as well as the effect of the duration of the measurement, a previously developed screw tribometer (depicted in Figure 1) was adapted. This figure shows the measurement setup for bulk density and tribological tests. The piston was pneumatically pressed onto the sample. The temperature of the shaft, the sample chamber, and the piston as well as the frictional velocity can be widely varied to simulate real processing conditions. The velocity can be chosen from 0.1 to 1.3 m·s<sup>-1</sup> and temperatures of up to 350°C are possible. The pressing device, powered by a pneumatic cylinder, is mounted with two big ball bearings at the same bearing axis as the test shaft. The

normal force, which is applied to the pellets, is measured by a load cell. The frictional force between the bulk polymer and the rotating shaft causes a torque at the complete pressing device. This torque is measured precisely with a second load cell. Due to this construction, measurement errors caused by friction in the bearings and thermal strains and forces caused by the pressing device can be avoided. This enables the accurate measurement of the frictional force.

The coefficient of friction is calculated from the frictional force and the measured normal force. The piston movement is measured with a position encoder which is integrated in the pneumatic cylinder. The shaft and the bulk polymer can be changed easily to enable the possibility of testing various plastics and shafts with different surfaces and coatings. The sample chamber's cross-sectional dimensions in the tests are 27 × 21 mm<sup>2</sup>. It was conditioned using six heating cartridges located in the walls of the chamber, providing 50 W each. The temperature was controlled and monitored with two thermocouples on opposite walls of the sample chamber. The shaft is made of the tool steel 1.2311 (40CrMnNiMo8-6-4), has a diameter of 100 mm, and is polished. It was heated using four 100 W heating cartridges. The surface temperature was measured using a thermocouple. The piston was conditioned with one 50 W heating cartridge which was monitored with one thermocouple in the piston (indicated by a small recess on top of the piston in Figure 1). The temperature of the piston, the sample chamber, and the shaft is regulated with a proportional-integral-derivative controller.

The bulk density tests were conducted at a temperature of 20, 60, 80, and 120°C, dynamically applying an apparent pressure of 4–35 bar. The dynamic pressure program is chosen because it relates best to the SSE process, where the pressure is built up dynamically as well. In every test, the sample chamber, the piston, the shaft, and the bulk solids were preheated to the designated temperature before filling 5 g of the polymer into the



**Figure 3.** Time dependency of the bulk densities of virgin pellets and long cylinders at a temperature of (a) 20°C, (b) 60°C, (c) 80°C, and (d) 120°C.

chamber through a funnel resulting in piston starting positions of about 17 mm for virgin pellets and 20 mm for long cylinders. The polymeric samples were preheated in a convection oven for approximately 20 min for every test, excluding those at a temperature of 20°C. The testing duration for each measurement was 55 s, after which the samples were removed and discarded.

The time dependency was studied by applying a constant apparent pressure of 4, 20, and 35 bar to 5 g of the bulk material, recording the piston position for the duration of 60 s at a temperature of 20, 60, 80, and 120°C.

Moreover, the effect of the filling quantities was examined, using 3 g (filling heights around 11 mm (virgin) and 13 mm (long cylinders)) or 7 g (filling heights around 23 mm (virgin) and 27 mm (long cylinders)) of the materials for tests with dynamically applied pressure from 4 to 35 bar at the same temperatures as before.

Since the bulk density is expected to deliver different values in a moving system, experiments with 5 g bulk material at a temperature of 20 and 120°C are done with constant pressure (4, 20, and 35 bar) and dynamic pressure increase (4–35 bar) and 0.1 m·s<sup>-1</sup> velocity of the shaft.

All the tests are repeated four times at each chosen condition. The bulk densities are then calculated from the weight of the sample and the piston position.

#### Investigation of the External Coefficient of Friction

These measurements were conducted using the same device as before, with the only difference that the shaft was rotated at a defined velocity (0.1 m·s<sup>-1</sup>) while applying the pressure (4, 20,

and 35 bar) to the bulk material in the conditioned sample chamber (temperatures of 20, 60 and 120°C). The chosen velocity relates well to the extrusion experiments in the previous study.<sup>3</sup> The polymer pellets are arranged in a monolayer, so the applied pressure is not reduced due to frictional forces at the sample chamber walls. The ECOF for 10 turns of the shaft is observed.

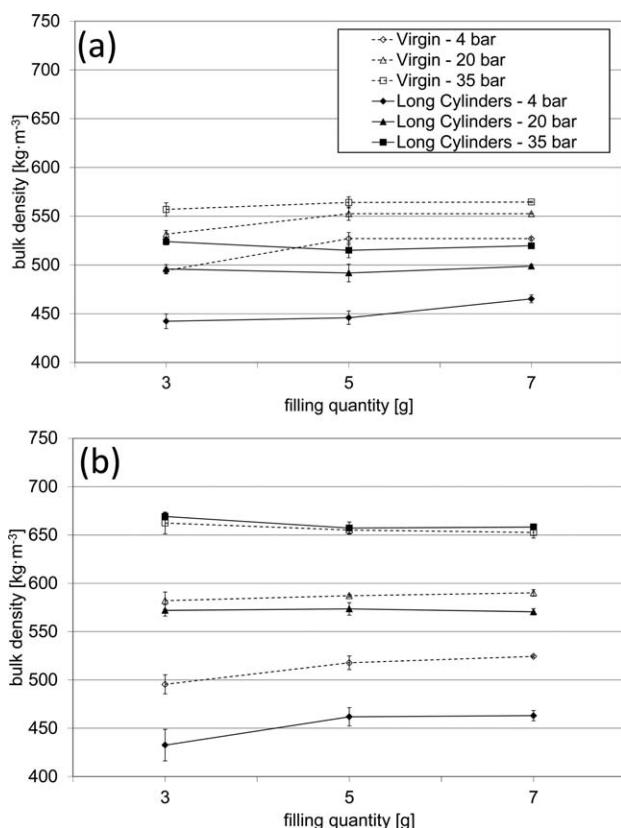
## RESULTS

### Determination of Solid Bulk Properties

The measurements at standard conditions according to EN ISO 60 deliver the value of  $514.80 \pm 1.81 \text{ kg}\cdot\text{m}^{-3}$  for the virgin material and  $422.80 \pm 3.43 \text{ kg}\cdot\text{m}^{-3}$  for the long cylinders.

The achieved results with 5 g of the materials and dynamically applied pressure at different temperatures are depicted in Figure 2. The bulk density of the long cylinders is low at first, but it increases with the pressure and/or the temperature. The spherical virgin pellets exhibit higher bulk densities at low pressure and temperature and the increase is not as high as for the cylindrical pellet shape. For this reason, the bulk density of the cylinders exceeds the values of the virgin material at a temperature of 120°C when a pressure of 35 bar is reached.

The time dependency of the bulk density of the two pellet geometries at constant applied pressure for a temperature of 20, 60, 80, and 120°C is shown in Figure 3. It can be observed that after a short time, a constant value is achieved in every experiment, proving that the method is reliable. The average bulk density values of the virgin pellets at 20°C temperature [Figure 3(a)] is 14.3% higher at 4 bar pressure, 8.6% higher at 20 bar, and 4.2% higher at 35 bar compared to the long cylinders. At a temperature of 60°C, the increase is 13.6% at a pressure of



**Figure 4.** Influence of the sample mass on the bulk density of virgin and long cylindrical pellets at a pressure of 4, 20, and 35 bar and a temperature of (a) 20°C and (b) 120°C.

4 bar, 7.0% at 20 bar, and 3.2% at 35 bar, respectively [Figure 3(b)]. When a temperature of 80°C is reached [Figure 3(c)], the corresponding values are 16.4, 5.7, and 1.4%, respectively. It can be observed that at 20 and 35 bar pressure, the difference between the bulk densities of the two pellet shapes decreases with higher temperature, whereas the values at a pressure of 4 bar applied pressure do not show a clear dependence on temperature. At a temperature of 120°C [Figure 3(d)], the bulk density of the virgin material is only higher at 4 bar pressure (13.1%), whereas at a pressure of 20 and 35 bar, the long cylindrical pellets exhibit a higher measured bulk density (0.9 and 5.9%, respectively).

Comparing the experiments with constant pressure and those where the pressure was applied dynamically, the maximum measured bulk density is 7.1% higher for long cylinders and 1.4% higher for virgin pellets when the material is compressed constantly for a duration of 60 s. Those maximum values account to a 66.8% increase for long cylinders and 29.3% increase for spheroidal pellets from the values derived from the standard measurement according to EN ISO 60.

It was also noticed that the long cylinders stick together when a pressure of 35 bar and a temperature of 120°C is reached and have to be loosened mechanically prior to being removed.

To determine the ramifications of the geometry of the sample chamber and the supporting effects of the sample chamber wall

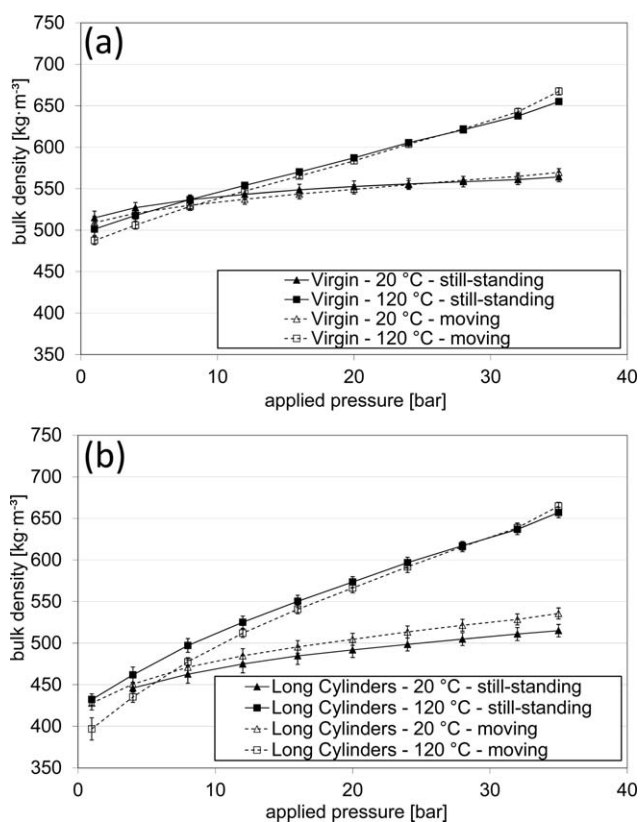
due to pressure reduction caused by frictional forces at the walls, experiments with different filling quantities of the materials were conducted.

The results of these tests, where the pressure of 4–35 bar was applied dynamically over the duration of 55 s, are shown in Figure 4 for a temperature of (a) 20°C and (b) 120°C.

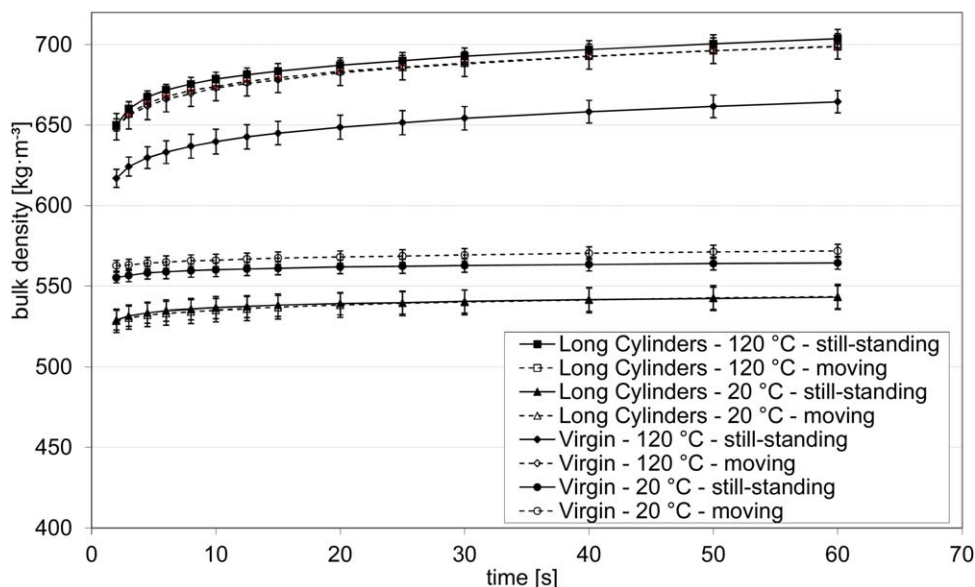
To give a better overview, only single values for a pressure of 4, 20, and 35 bar are plotted.

Those experiments prove that no significant influence of the initial weight can be proven at any given set of parameters. The density is lower at the walls of the sample chamber, than in its center resulting from voids between the straight wall and the granular bulk solids. Therefore, the determined bulk density is mostly lower when using less material. The bulk of spheroidal virgin pellets contains a higher proportion of voids, so the measured bulk density seems more sensitive to the filling quantity which can be seen in Figure 4. At high temperature and high pressure, this effect seems to become negligible as different filling quantities exhibit very similar bulk densities.

Apart from this, a comparison between the bulk density values for a still standing and a moving shaft with dynamically applied pressure was performed. This is carried out for a temperature of 20 and 120°C in Figure 5 where (a) represents the virgin material and (b), the long cylinders. At a temperature of 120°C,



**Figure 5.** Comparison of the measured bulk density using a still-standing and a rotating shaft for (a) virgin and (b) long cylindrical pellets at a temperature of 20 and 120°C with dynamically applied pressure from 4 to 35 bar over a duration of 55 s.



**Figure 6.** Development of the bulk densities of virgin and long cylindrical pellets at constant pressure of 35 bar at a temperature of 20 and 120°C comparing measurements between a still-standing and a rotating shaft.

there is almost no difference in the measured densities. This is also true for the virgin material at a temperature of 20°C. The long cylinders exhibit a higher density at a temperature of 20°C when the shaft is moving.

These investigations were also conducted with a static load on the material for a duration of 60 s. A comparison between tests with a moving and a still-standing shaft at a temperature of 20 and 120°C and a pressure of 35 bar can be seen in Figure 6. On one hand, the difference between the bulk densities of long

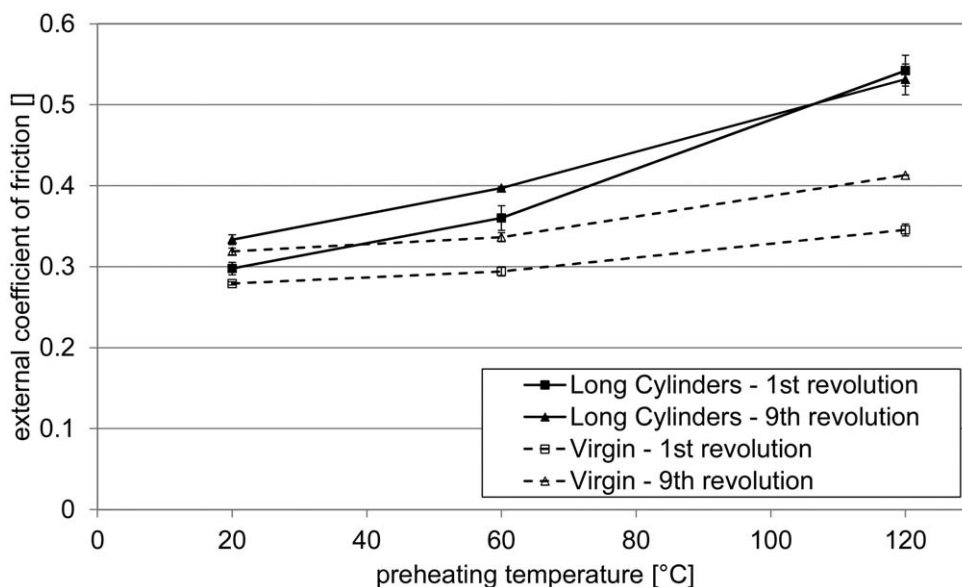
cylinders is only marginal and within the standard deviations of the values. The virgin material, on the other hand, exhibits higher bulk densities with a rotating shaft. At low temperatures, the increase is around 1.5%; but at a temperature of 120°C, it accounts to as much as 5.3% and has almost reached the value of the bulk density of long cylindrical pellets.

#### Investigation of the External Coefficient of Friction

The ECOF shows a strong dependence on the pressure and the temperature. As the interface temperature is increasing during

**Table II.** ECOF Between the Shaft and the Virgin Material and the Long Cylinders After the First and the Ninth Revolution of the Shaft Including Their Standard Deviations ( $\sigma$ ) at a Pressure of 4, 20, and 35 bar and a Preheating Temperature of 20, 60, and 120°C

Temperature [°C]	Virgin—4 bar—1 <sup>st</sup> revolution		Virgin—4 bar—9 <sup>th</sup> revolution		Long cylinders—4 bar—1 <sup>st</sup> revolution		Long cylinders—4 bar—9 <sup>th</sup> revolution	
	ECOF	$\sigma$	ECOF	$\sigma$	ECOF	$\sigma$	ECOF	$\sigma$
20	0.288	0.018	0.337	0.023	0.293	0.011	0.348	0.009
60	0.296	0.009	0.325	0.013	0.392	0.007	0.434	0.001
120	0.322	0.023	0.385	0.032	0.579	0.029	0.598	0.015
[°C]	Virgin—20 bar—1 <sup>st</sup> revolution		Virgin—20 bar—9 <sup>th</sup> revolution		Long cylinders—20 bar—1 <sup>st</sup> revolution		Long cylinders—20 bar—9 <sup>th</sup> revolution	
	ECOF	$\sigma$	ECOF	$\sigma$	ECOF	$\sigma$	ECOF	$\sigma$
20	0.279	0.002	0.319	0.004	0.298	0.008	0.333	0.006
60	0.294	0.006	0.336	0.005	0.360	0.015	0.397	0.001
120	0.345	0.007	0.413	0.000	0.542	0.019	0.531	0.019
[°C]	Virgin—35 bar—1 <sup>st</sup> revolution		Virgin—35 bar—9 <sup>th</sup> revolution		Long cylinders—35 bar—1 <sup>st</sup> revolution		Long cylinders—35 bar—9 <sup>th</sup> revolution	
	ECOF	$\sigma$	ECOF	$\sigma$	ECOF	$\sigma$	ECOF	$\sigma$
20	0.284	0.007	0.318	0.005	0.279	0.012	0.320	0.007
60	0.306	0.003	0.346	0.008	0.368	0.004	0.399	0.019
120	0.349	0.032	0.384	0.008	0.427	0.014	0.402	0.007



**Figure 7.** ECOF between the shaft and the virgin material and the long cylinders after the first and the ninth revolution of the shaft at a pressure of 20 bar and a preheating temperature of 20, 60, and 120°C.

the measurements through frictional heat, the values are not constant over the entire duration. For this reason, the results for the first and the ninth revolution of the shaft are presented (Table II).

At a temperature of 20°C, the ECOF of the long cylinders is only slightly higher than the one of the virgin material at the chosen rotational speed of  $0.1 \text{ m}\cdot\text{s}^{-1}$ . With increasing temperature, the ECOF of the long cylindrical pellets shows a significant increase, whereas the ECOF of the virgin material is only slightly higher at those conditions.

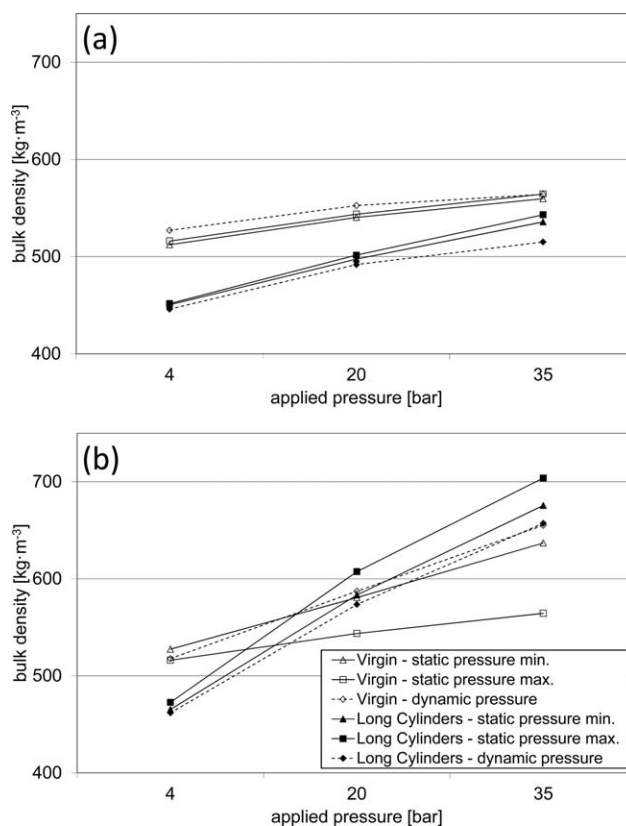
The most significant increase is exhibited by the long cylinders after the first revolution of the shaft at 4 bar comparing temperatures of 20 and 120°C when it accounts to 100%. The maximum raise of the ECOF for the virgin material is after the ninth revolution at a pressure of 20 bar comparing temperatures of 20 and 120°C when it reaches 28%.

Figure 7 depicts the ECOF at a pressure of 20 bar where the temperature dependency is clearly shown. There is an irregularity at a temperature of 120°C when conducting experiments with the long cylindrical pellets, as the ECOF decreases with the frictional distance. This is due to the formation of melt film at the interface, resulting from the frictional heat. Apart from that, the figure clearly shows the higher possible ECOF when using the long cylinders.

## DISCUSSION

The data received from the performed experiments at standard conditions would suggest that the virgin pellets should exhibit a higher mass flow rate in the extrusion process due to a far higher bulk density. Yet, it can be shown that if the temperature and the pressure are increased, the bulk density of the long cylindrical pellets can exceed one of the virgin granules. In general, the bulk density rises with the temperature and the pressure in every experiment.

The time and pressure dependency of the bulk density was also shown by Hyun and Spalding.<sup>30</sup> Their experiments were made for different polymeric materials, but did not consider different pellet shapes (except for a comparison between powder and pellets). They concluded that for semicrystalline thermoplastic materials,



**Figure 8.** Comparison between bulk densities at constant pressure (min and max values) and those, where the pressure was applied dynamically for (a) 20°C and (b) 120°C.

the pressure dependency can be proven for every test above the glass transition temperature  $T_g$ . This was also observed in this study.

The fact that the bulk density shows no real correlation with the tested sample mass could mean that the pressure loss from the top of the sample to the shaft due to friction at the chamber wall is either negligible or identical for every sample mass tested at those conditions.

The bulk density of the long cylindrical pellets exhibits almost no divergence between the tests with a still-standing and a moving shaft. A possible explanation is that in this rather small enclosing sample chamber, almost no relative movement between the long pellets is possible. This can be quite different in an extruder with a relatively large screw channel compared to the pellet size. The virgin pellets show a different behavior, as the bulk density rises when the shaft is moving. The spheroidal shape of the pellets proves to be an advantage here, as movement of individual pellets is not hindered as much as for long cylinders.

The comparison between the two chosen pressure programs is made in Figure 8 for a temperature of 20 and 120°C. The experiments with dynamically applied pressure always provide results smaller than both minimum and maximum values for the bulk density of long cylinders at constant pressure. The opposite is observed for the virgin material at a temperature of 20°C. At a temperature of 120°C, the dynamic pressure program yields a smaller bulk density at a pressure of 4 bar, which then lies between the minimum and maximum of the constant program at a pressure 20 and 35 bar. Constant pressure over a longer duration obviously leads to a higher compression for long cylinders, possibly due to higher deformation, whereas the virgin material cannot be deformed as easily.

A vital aspect of the good compressibility of the long cylinders is their relatively small diameter, compared to the virgin pellets. Through this, deformation can take place more easily, especially at elevated temperature as the tensile modulus decreases. This can be seen in the experiments at a temperature of 80°C. The datasheet provides a heat deflection temperature of 88°C for load of 0.45 N·mm<sup>-2</sup> (corresponding to 4.5 bar). It can be assumed that for higher pressure, 80°C is high enough to allow the material to be deformed under the applied load and thereby increasing the density by filling empty spots in the bulk.

The measurements of the ECOF show a strong dependence on the pressure, temperature, and frictional distance. This was also reported by Spalding and Hyun when doing experiments with different polyethylene grades. They found that an increase in pressure delivers smaller coefficients of friction due to a nonlinear relationship between the real contact area and the normal force when working with polymeric materials. According to their research, the temperature plays an undefinable role, leading to complex functions for different materials. Due to the interference of different effects, the ECOF can either increase or decrease with rising temperature in their work.<sup>21</sup>

In this study, the effect of the temperature is very clear as increasing temperatures always lead to higher coefficients of friction. Increasing the pressure delivers smaller ECOF values. The most

important finding is that the ECOF is dependent on the pellet shape as the coefficients are always higher for long cylinders compared to the virgin material. This contradicts Gamache *et al.* who observed no significant correlation between the ECOF and the pellet shape when doing experiments with polypropylene cylinders and flattened cylinders.<sup>22</sup> Yet, the ECOF presented in their work is between 0.2 and 0.6, which is comparable to this study.

The significant rise in bulk density combined with the higher ECOF at elevated temperature and pressure gives the long cylinders an advantage over virgin pellets in the extrusion process. In the previously performed extrusion experiments, the long cylinders exhibit their potential for compression as the screw-cool and pull-out tests show.<sup>3</sup> Heavy deformation of the pellets takes place in the first turns of the screw leading to high pressure and fast melting. The corresponding mass flow rate values are always higher for long cylinders than for the virgin material. There is a clear drop in pressure at the end of the solids conveying zone when accelerating the screw while processing the long cylinders. This might be due to the fact that the feeding behavior works better at low screw speeds, which was also found by Wortberg and Rahal and Lessmann *et al.*<sup>14,25,32</sup> This would also explain the higher mass flow rate increase at lower screw speeds in comparison with the virgin pellets. Another reason for this could be that the faster movement of the screw leads to a higher compression of the virgin pellets (as shown in Figure 6) that could not be achieved with the long cylindrical pellets.

It is obvious that the pressure and the temperature in the extruder exceed those in the bulk density experiments. Higher temperatures, on one hand, would not have been possible though as melting of the material in the sample chamber would deliver incorrect solid bulk density values. The maximum pressure, on the other hand, was limited by the equipment.

## CONCLUSIONS

In conclusion, it could be demonstrated that different pellet shapes of the same grade exhibit diverging bulk properties which are strongly dependent on the ambient conditions of the system. Long cylindrical pellets appear nonbeneficial for the extrusion process at standard conditions. This changes dramatically when the pressure and the temperature are rising. The bulk density then exceeds the one of the spheroidal virgin pellets. Combined with the higher detected ECOF, a high compression and fast heating and melting of the material in the extruder can be achieved, which then leads to a significant rise in the mass flow rate.

## ACKNOWLEDGMENTS

Financial support for this work was provided by the Austrian Research Promotion Agency—FFG within the project “Plastsurf” in the framework of the funding program COIN-Aufbau.

## REFERENCES

1. Markarian, J.; *Plastics, Additives and Compounding* **2004**, *6*, 4, 22.
2. Potente, H.; Schöppner, V. *Int. Polym. Process.* **1995**, *10*, 1, 10.



3. Längauer, M.; Liu, K.; Kneidinger, C.; Schaffler, G.; Purgleitner, B.; Zitzenbacher, G. *J. Appl. Polym. Sci.* **2015**, *132*, 41716.
4. Campbell, A. G.; Spalding, M. A. *Analyzing and Troubleshooting Single-Screw Extruder*; Hanser Publishers: Munich, **2013**; Chapter 6, p 238.
5. Sikora, J. W. *Int. Polym. Process.* **2014**, *29*, 412.
6. Darnell, W. H.; Mol, E. A. *J. SPE J.* **1956**, *12*, 20.
7. Schneider, K. *Der Fördervorgang in der Einzugszone eines Extruders*, Ph.D. thesis; RWTH-Aachen: Germany, **1968**.
8. Broyer, E. Z.; Tadmor, Z. *Polym. Eng. Sci.* **1974**, *14*, 589.
9. Campbell, G. A.; Dontula, N. *Int. Polym. Process.* **1995**, *10*, 30.
10. Grünschloß, E. *Kunststoffe* **1984**, *74*, 480.
11. Rauwendaal, C. *Polymer Extrusion*, 4<sup>th</sup> ed.; Hanser Publishers: Munich, **2001**; Chapter 7.2.2, p 223.
12. Yung, K. L.; Xu, Y.; Lau, K. H. *Int. Polym. Process.* **2002**, *17*, 91.
13. Potente, H.; Pohl, T. *Int. Polym. Process.* **2002**, *17*, 11.
14. Leßmann, J.-S.; Weddige, R.; Schöppner, V.; Porsch, A. *Int. Polym. Process.* **2012**, *27*, 469.
15. Moysey, P. A.; Cloet, K. L.; Thompson, M. R. *Int. Polym. Process.* **XXII** **2008**, *3*, 301.
16. Michelangelli, O. P.; Gaspar-Cunha, A.; Covas, J. A. *Powder Technol.* **2014**, *264*, 401.
17. Michelangelli, O. P.; Yamanoi, M.; Gaspar-Cunha, A.; Covas, J. A. *Proc. Inst. Mech. Eng. Part E J. Process Mech. Eng.* **2011**, *225*, *4*, 255.
18. Mayer, T. *Proceedings of the 14<sup>th</sup> Leobner Kunststoffkolloquium*, Leoben, Austria, **1996**, 18/1.
19. Chung, C. I.; Hennessey, W. J.; Tusim., M. H. *Polym. Eng. Sci.* **1977**, *17*, 9.
20. Spalding, M. A.; Kirkpatrick, D. E.; Hyun, K. S. *Polym. Eng. Sci.* **1993**, *33*, 423.
21. Spalding, M. A.; Hyun, K. S. *Polym. Eng. Sci.* **1995**, *35*, 557.
22. Gamache, E.; Lafleur, P. G.; Peiti, C.; Vergnes, B. *Polym. Eng. Sci.* **1999**, *39*, 1604.
23. Hennes, J. P. *Determination of Material Indices and Simulation of the Processes in the Feed Section of Conventional Single-Screw Extruders*, Ph.D. thesis; RWTH-Aachen: Germany, **2000**.
24. Zitzenbacher, G.; Langecker, G. R.; Schatzer, R. *Kunststoffe plast europe* **2005**, Nr. 4, 43.
25. Wortberg, J.; Rahal, H. *J. Plast. Technol.* **2007**, *3*, 1.
26. Kleineheismann, S.; Potente, H. *J. Plast. Technol.* **2009**, *5*, 201.
27. Miethlinger, J. *Kunststoffe* **2003**, *4*, 49.
28. Jia, M.-Y.; Pan, L.; Xue, P.; Wang, K.-J.; Jin, X.-M. *Int. Polym. Process.* **2013**, *28*, 267.
29. Langecker, G. R.; Binder, W.; Zitzenbacher, G. *Österreichische Kunststoffzeitschrift* **2002**, *33*, 46.
30. Hyun, K. S.; Spalding, M. A. *Polym. Eng. Sci.* **1990**, *30*, 571.
31. Zitzenbacher, G.; Kneidinger, C.; Kögler, A. *Österreichische Kunststoffzeitschrift* **2009**, *3/4*, 53.
32. Lessmann, J.-S.; Weddige, R.; Schöppner, V.; Porsch, A. *Kunststoffe plast europe* **2012**, Nr. 5, 72.